

SUPPORTING INFORMATION

Influence of the [4Fe-4S] Cluster Coordinating Cysteines on Active Site Maturation and Catalytic Properties of *C. reinhardtii* [FeFe]-Hydrogenase

Leonie Kertess,^a Agnieszka Adamska-Venkatesh,^b Patricia Rodriguez-Maciá,^b Olaf Rüdiger,^b Wolfgang Lubitz^b and Thomas Happe^{a*}

^a AG Photobiotechnologie, Lehrstuhl für Biochemie der Pflanzen, Ruhr Universität Bochum, Universitätsstr. 150, 44801 Bochum, Germany.

^b Max Planck Institute for Chemical Energy Conversion, Stiftstrasse 34-36, 45470 Mülheim an der Ruhr, Germany.

* To whom correspondences should be addressed: Prof. Dr. Thomas Happe, AG Photobiotechnologie, Lehrstuhl für Biochemie der Pflanzen, Ruhr Universität Bochum, Universitätsstr. 150, 44801 Bochum, Germany. E-mail: thomas.happe@rub.de, Phone: +49 (0) 23 43 22 70 26.

Table S1: Mutagenic primers used in this study.

Table S2: Iron content of apoHydA1 and holoHydA1 variants after 1 h and 30 h *in vitro* maturation.

Table S3: Summary of the relevant redox states.

Figure S1: Spectroscopic characterization of apoHydA1 "A" and "D" variants.

Figure S2: *In vivo* maturation and oxidation screening of holoHydA1 variants.

Figure S3: Annotated FTIR spectra of holoHydA1 variants.

Figure S4: Comparison of normalized FTIR spectra of holoHydA1 variants after 1 h and 30 h *in vitro* maturation.

Figure S5: *In vitro* maturation followed by FTIR over 30 h.

Figure S6: Comparison of cyclic voltammograms of holoHydA1 variants from pH 5 to pH 10.

Scheme S1: Schematic summary of the influence of the [4Fe-4S] Cluster Coordinating Cysteines.

Table S1: Mutagenic primers used in this study.

Name	Sequence 5' – 3' ^a	nt
C115A_for	CAGCTGC g cgCCGGGCTGGATTGCGATG	28
C115A_rev	CAGCCCG G cgGCAGCTGGTAAACATCG	28
C115D_for	CAGCTGC g atCCGGGCTGGATTGCGATG	28
C115D_rev	CAGCCCG G atcGCAGCTGGTAAACATCG	28
C115S_for	CAGCTGC CaG CCCGGGCTGGATTGCGATG	28
C115S_rev	CAGCCCG GG CtGCAGCTGGTAAACATCG	28
C170A_for	CATTATGCC G cgACCCGTAAACAGAGCGAAG	32
C170A_rev	GTTTACGGG T cgCGGCATAATGCTCACCATC	32
C170D_for	CATTATGCC g atACCCGTAAACAGAGCGAAG	32
C170D_rev	GTTTACGGG T atcCGGCATAATGCTCACCATC	32
C170S_for	CATTATGCC GaG ACCCGTAAACAGAGCGAAG	32
C170S_rev	GTTTACGGG T GcCGGCATAATGCTCACCATC	32
C362A_for	GAAATTATGGCG g cgCCGGCGGGCTGCGTGGG	32
C362A_rev	GCCCGCC G cgCGCCATAATTTCCACAAAATC	33
C362D_for	GAAATTATGGCG g atCCGGCGGGCTGCGTGGG	32
C362D_rev	GCCCGCC G atcCGCCATAATTTCCACAAAATC	33
C362S_for	GAAATTATGGCG CaG CCCGGCGGGCTGCGTGGG	32
C362S_rev	GCCCGCC GG CtCGCCATAATTTCCACAAAATC	33
C366A_for	GCGGG C cgGTGGGCGGCGGGCGGCCAG	27
C366A_rev	CGCCGCC C AcgcGCCCGCCGGGCACG	27
C366D_for	GCGGG C gatGTGGGCGGCGGGCGGCCAG	27
C366D_rev	CGCCGCC C atcGCCCGCCGGGCACG	27
C366S_for	GCGGG CaG CGTGGGCGGCGGGCGGCCAG	27
C366S_rev	CGCCGCC CG CtGCCCGCCGGGCACG	27

^a Lower case letters represent modifications relative to the WT sequence. Mutated codons resulting in amino acid exchanges are written in bold.

Table S2: Iron content of apoHydA1 and holoHydA1 variants based on the method of Fish in [mol/mol] after 1 h and 30 h of *in vitro* maturation. Determined in triplicates from samples prepared for FTIR spectroscopy and activity measurements.

Sample	1 h maturation			30 h maturation		
	Iron/apo HydA1	Iron/holo HydA1	Increase ^a	Iron/apo HydA1	Iron/holo HydA1	Increase
WT	3.84 ± 0.01	5.30 ± 0.08	1.46	4.19 ± 0.13	5.46 ± 0.09	1.27
C170A	2.86 ± 0.13	3.43 ± 0.46	0.57	3.31 ± 0.17	4.72 ± 0.97	1.41
C170D	2.69 ± 0.14	3.55 ± 0.07	0.86	2.64 ± 0.20	5.14 ± 0.29	2.50
C170S	2.13 ± 0.02	2.76 ± 0.02	0.63	2.68 ± 0.09	3.92 ± 0.12	1.24
C362A	1.94 ± 0.03	2.71 ± 0.47	0.77	1.10 ± 0.07	2.96 ± 0.88	1.86
C362D	0.86 ± 0.06	1.79 ± 0.10	0.93	1.12 ± 0.10	2.91 ± 0.09	1.79
C362S	1.78 ± 0.05	2.91 ± 0.13	1.13	1.99 ± 0.07	2.70 ± 0.04	0.71

^a Adding the chemically synthesized [2Fe]^{MIM} cluster to the apoHydA1 not only matures the proteins'

[2Fe] site but also the [4Fe-4S] site. Potential free iron ions from degrading [2Fe]^{MIM} cofactor may reconstitute under the reductive conditions present during the *in vitro* maturation process not fully occupied [4Fe-4S] clusters. This leads to an apparent increase of iron/HydA1 ratio even if the [2Fe]^{MIM} cluster is not integrated.

Table S3: Summary of relevant redox states of HydA1 WT.

Redox species	Wavenumber / cm ⁻¹			Electronic configuration		Altern. Annotation ^b
	CN	CO	μCO	[4Fe-4S]	[2Fe] ^a	
H _{ox}	2088/2072	1964/1940	1800	+2	I/II	-
H _{red}	2083/2069	1962/1933	1791	+1	I/II	Hred'
H _{red} H ⁺	2071/2032	1968/1914/1891	-	+2	I/I	Hred
H _{sred} H ⁺	2067/2027	1953/1917/1882	-	+1	I/I	-
H _{ox} -CO	2092/2084	2013/1970/1964	1810	+2	I/II	-
H _{red} '-CO	2086/2075	2002/1967/1951	1793	+1	I/II	-

^a Formal charge is given for Fe_p/Fe_d. ^b M. Senger, S. Mebs, J. Duan, O. Shulenina, K. Laun, L. Kertess, F. Wittkamp, U.-P. Apfel, T. Happe, M. Winkler, M. Haumann and S.T. Stripp, *Phys. Chem. Chem. Phys.*, 2017.

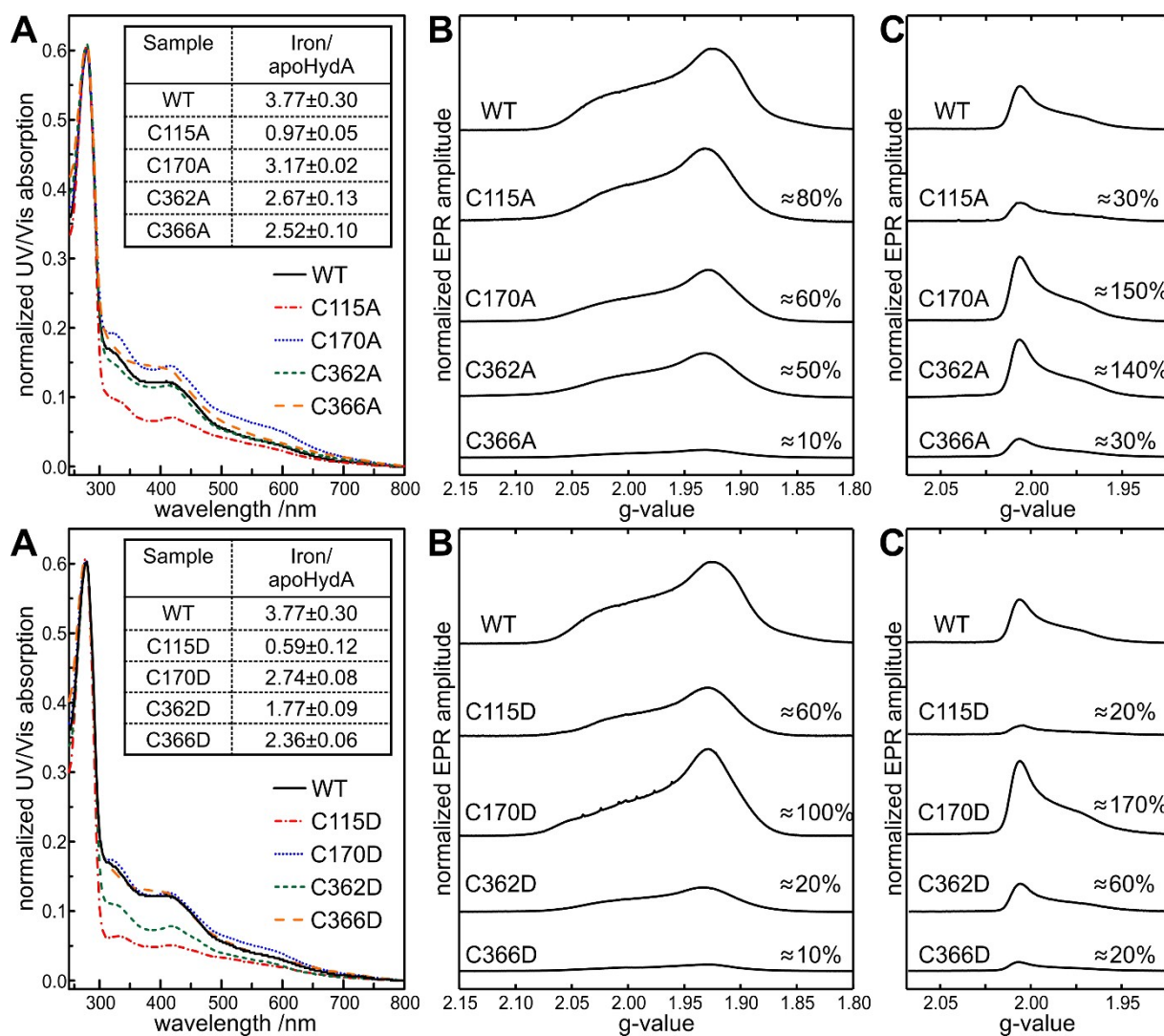


Figure S1: Spectroscopic characterization of apoHydA1 “A” and “D” variants. UV/vis absorbance spectra of apoHydA1 WT and the apoHydA1 C115A (red), C170A (blue), C362A (green) and C366A (orange) variants (top) as well as the apoHydA1 C115D (red), C170D (blue), C362D (green) and C366D (orange) variants (bottom) in their oxidized form. UV/vis spectra were measured at 25 °C in 100 mM Tris-HCl buffer, pH 8.0. Spectra were normalized to protein absorbance peak at 280 nm. Inset shows iron content of apoHydA1 variants based on the method of Fish in [mol/mol] determined in triplicate (A). Q-band FID detected EPR spectra obtained from the reduced (B) and oxidized (C) form of the apoHydA1 variants measured at 10 K and 20 K respectively. Ratio of variant to WT integral value is given in [%] with 10 to 20 % accuracy.

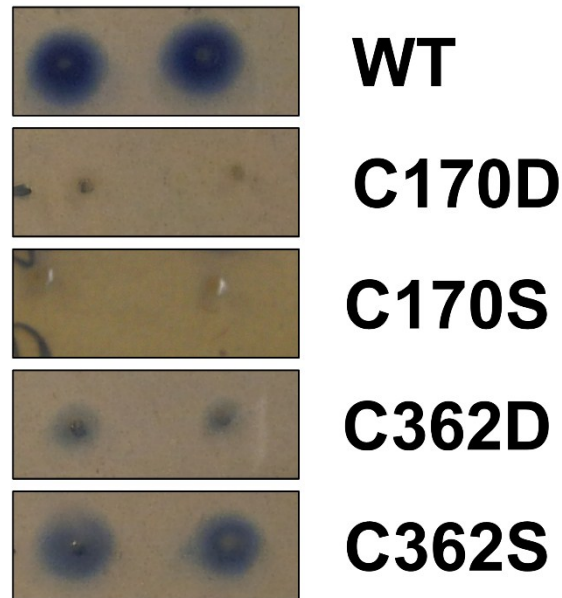


Figure S2: *In-vivo* maturation and oxidation screening of holoHydA1 variants. Colonies developed a blue color due to H₂-driven reduction of MV only if matured *in vivo* and sufficiently active in H₂ oxidation. Variants C170D and C170S are negative (colorless), while variants C362D and C362S show accumulation of reduced MV (blue). As positive control, a colony expressing holoHydA1 WT was plated.

***In vivo* maturation and hydrogen oxidation screening.** In order to obtain *in vivo* matured HydA1, pET-21(b)-hyda1 plasmid coding for HydA1 or one of its variants was co-transformed with the maturation plasmid pACYCDuet-1-hydGX-hydEF into *Escherichia coli* strain BL21(DE3) Δ iscR. Single colonies were transferred to LB-Agar plates supplemented with 100 mM MOPS/NaOH (pH 7.4), 25 mM sodium fumarate, 0.5 % glucose, and 2 mM ferric ammonium citrate as well as the antibiotics kanamycin (40 mg/mL), chloramphenicol (25mg/mL) and ampicillin (100 mg/mL) in analogy to the liquid medium used for apoHydA1 expression. Once single colonies had a diameter of roughly 3 mm, plates were transferred into an anaerobic environment (2 % H₂/ 98 % N₂) and protein expression was induced by adding dropwise 2 μ L of 5 mM Isopropyl- β -D-thiogalactopyranosid in 500 mM L-cystein per colony. After incubation for 20 h at room temperature enzymatic activity was assayed by adding dropwise 2 μ L of MV per colony prior to an incubation under 10 % H₂/ 90 % N₂ atmosphere for 10 min. Colonies eventually turned blue due to specific reduction of MV by HydA1 WT and variants performing H₂ oxidation under the given conditions.

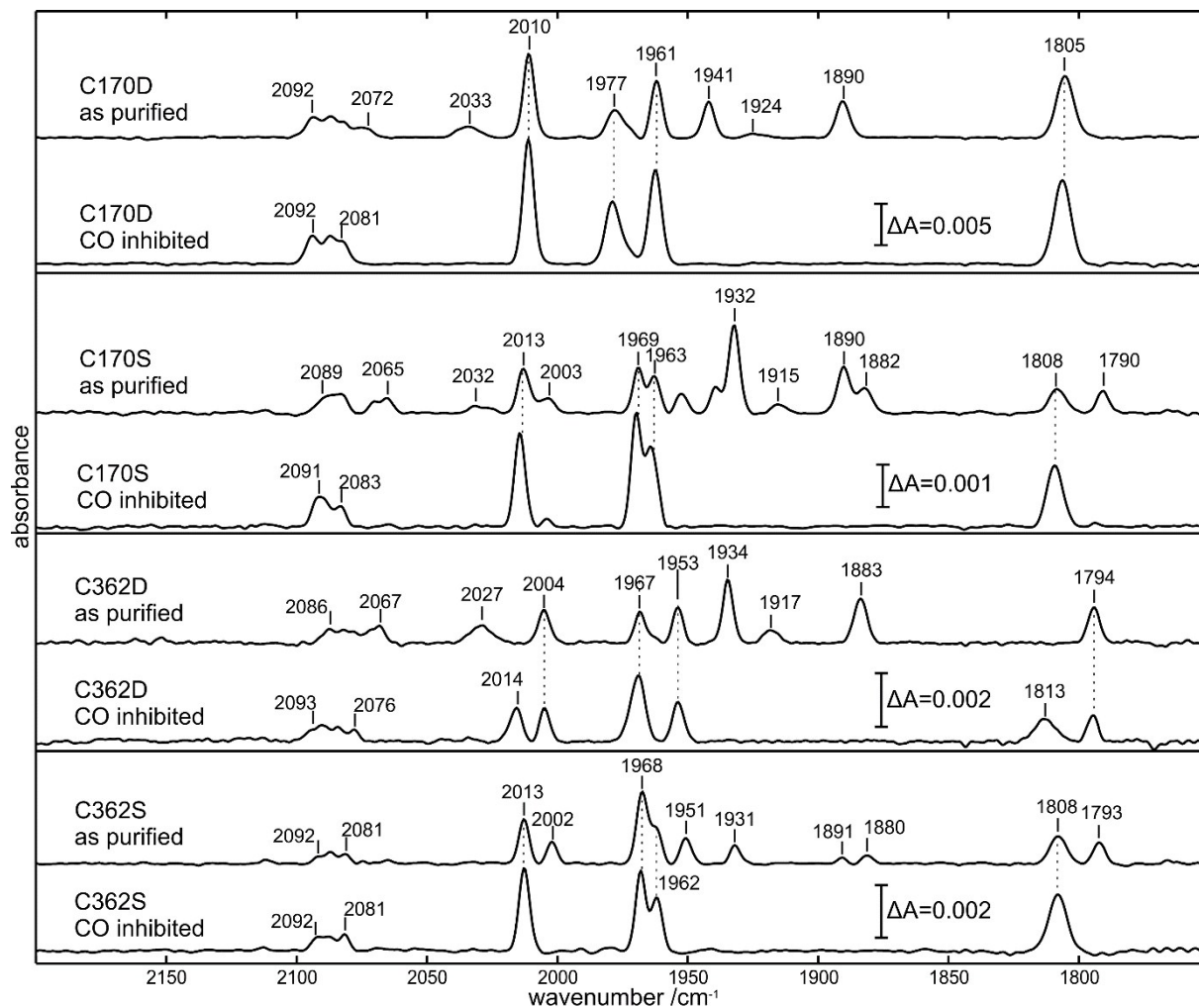


Figure S3: Annotated FTIR spectra of holoHydA1 variants. Spectra of C170D, C170S, C362D, and C362S variants without further treatment (“as purified”) and after 15 min CO flushing (“CO-inhibited”). Representative spectra of *in vitro* matured C170S and C362S samples for 30 h and C170D and C362D for 1 h. Sample concentration varied between 1 and 2.1 mM. Spectra were measured at 15 °C in 100 mM Tris-HCl buffer (pH 8) with 2 mM NaDT.

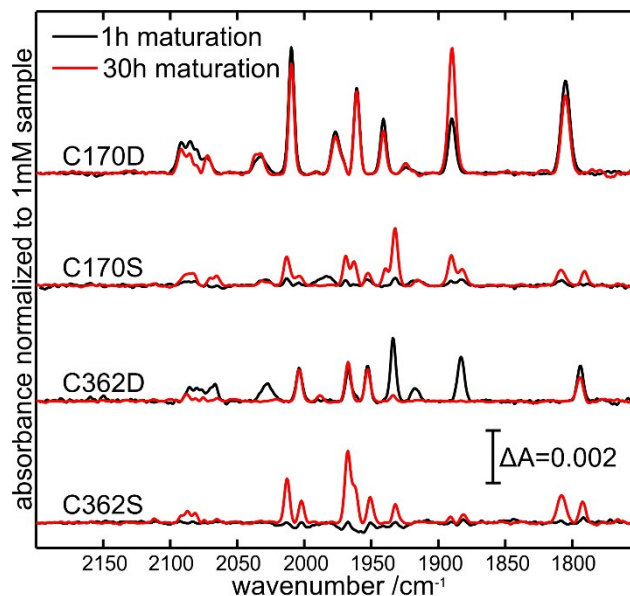


Figure S4: Comparison of normalized FTIR spectra of holoHydA1 variants after 1 h and 30 h *in vitro* maturation. FTIR spectra of holoHydA1 variants without further treatment after 1 h (black) and 30 h (red) *in vitro* maturation. Spectra were normalized to the same enzyme concentration (1 mM). Spectra were measured at 15 °C in 100 mM Tris-HCl buffer (pH 8) with 2 mM NaDT. Sample concentration varied between 0.7 and 2.1 mM.

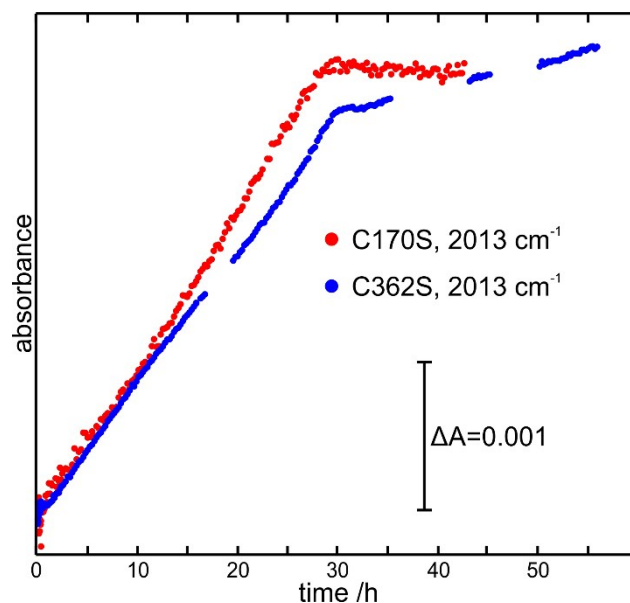


Figure S5: *In vitro* maturation followed by FTIR over 30 h. A 5-fold molar excess of $[2Fe]^{MIM}$ was used and maturation followed at 2013 cm^{-1} . Spectra were measured at 25 °C in 100 mM Tris-HCl buffer (pH 8) with 2 mM NaDT. Sample concentration were 1 and 0.8 mM for C170S and C362S, respectively.

***In vitro* maturation followed by FTIR spectroscopy.** A 5-fold molar excess of $[2Fe]^{MIM}$ was added to 800-1000 μM apoHydA1 in 100mM 100 mM Tris-HCl buffer (pH 8) with 2 mM NaDT initiating the maturation process. Sample was closed in the transmission FTIR cell and transferred to FTIR spectrometer where maturation process was constantly followed at 2013 cm^{-1} . Spectra were detected at 25 °C. Initially, spectra were accumulated for 100 (80 s) then 500 (6.5 min) and finally 1000 scans (around 13 min).

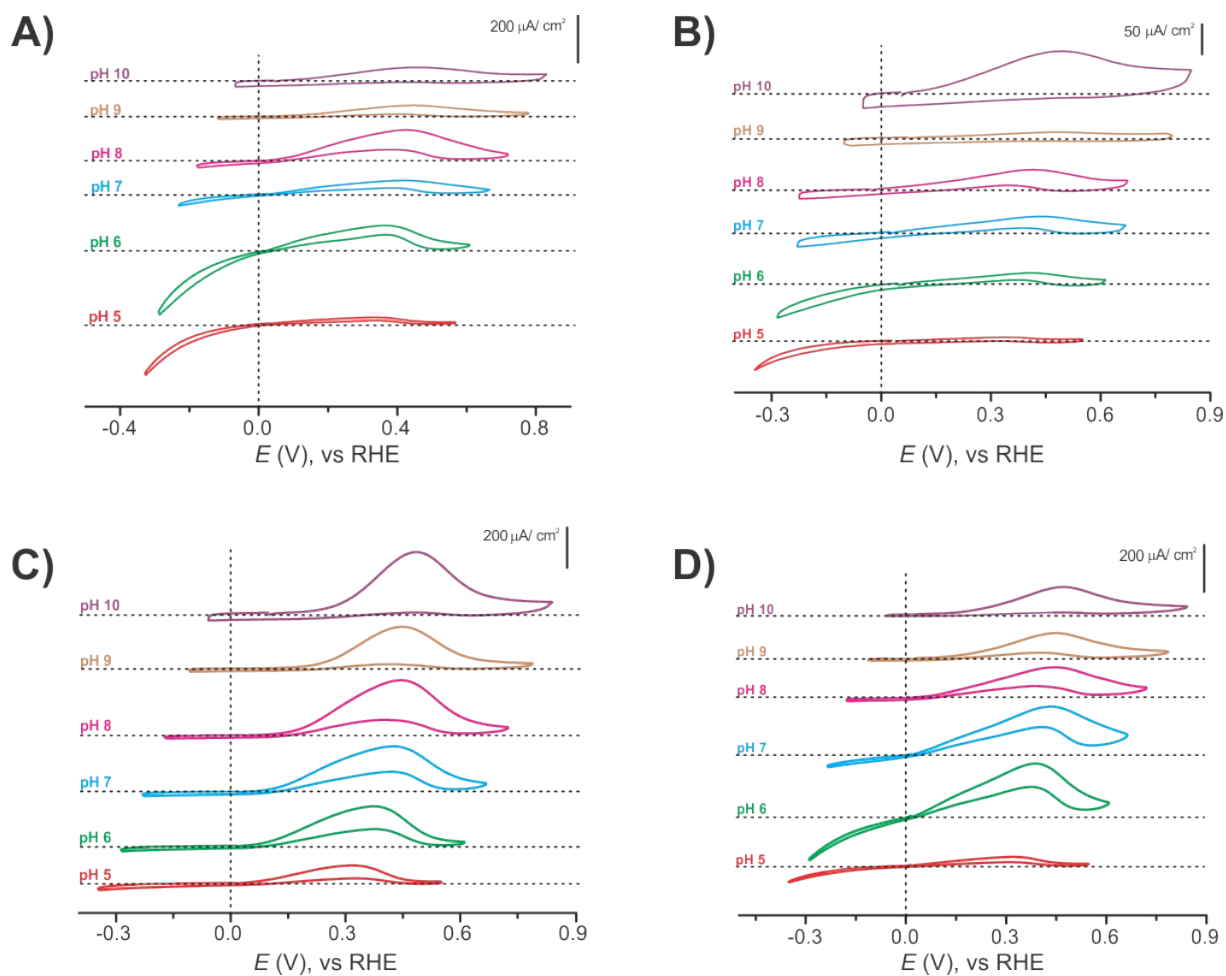
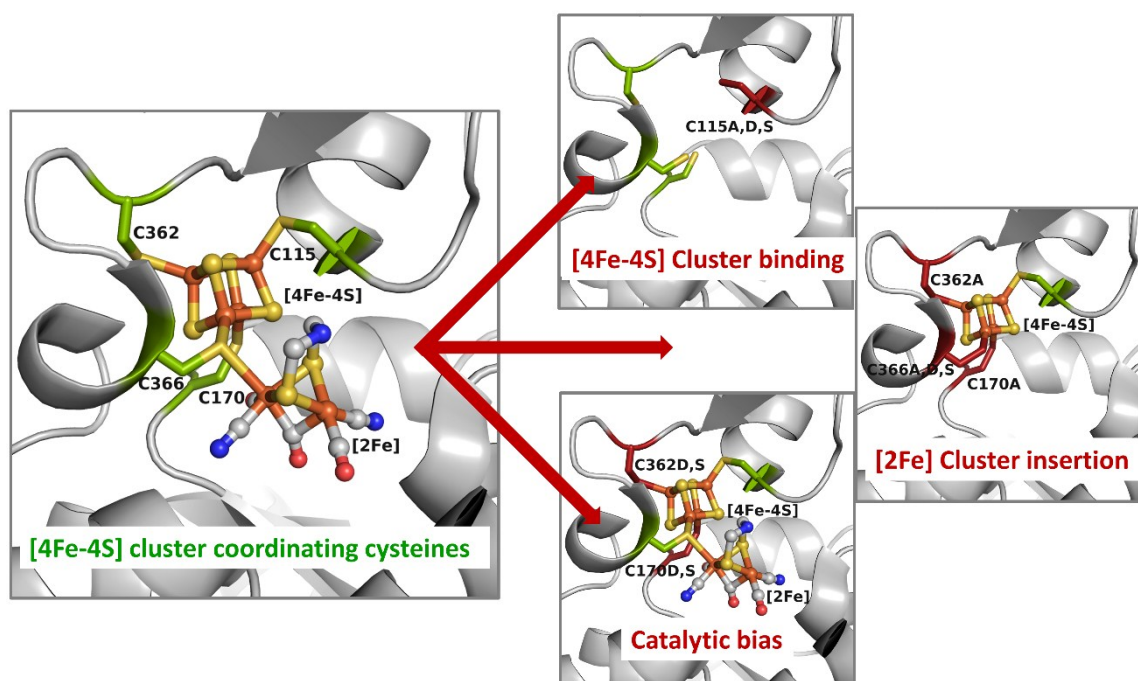


Figure S6: Comparison of cyclic voltammograms of holoHydA1 variants measured at different pH values (from pH 5 to pH 10). Cyclic voltammograms of holoHydA1 variants C170D (A), C170S (B), C362D (C) and C362S (D). The current density (y-axis) is plotted against the potential of the reversible hydrogen electrode (RHE) (x-axis) in order to show how the overpotential changes with the pH. Horizontal dotted lines represent the zero current and vertical dotted lines indicate the zero overpotential for all the pH values. The 4 variants were also measured at pH 4 but any of them showed catalytic current (not shown). All experimental conditions were the same as in Fig. 4 of the main text.



Scheme S1: Schematic summary of the influence of the [4Fe-4S] Cluster Coordinating Cysteines on Active Site Maturation and Catalytic Properties of *C. reinhardtii* [FeFe]-Hydrogenase. Cysteine residues coordinating the [4Fe-4S] cluster are shown as sticks in green and highlighted in brick red (numbering according to the expressed amino acid sequence). Protein Data Bank structures 3C8Y and 3LX4 were used for generating this model in PyMOL. Color coding is as follows: orange, iron; yellow, sulfur; gray, carbon; blue, nitrogen; red, oxygen.